IEEE Photonics Journal
An IEEE Photonics Society Publication

Open Access

Mode-Locked All-Fiber Lasers at Both Anomalous and Normal Dispersion Regimes Based on Spin-Coated MoS_2 Nano-Sheets on a Side-Polished Fiber

Volume 7, Number 1, February 2015

Reza Khazaeinezhad
Sahar Hosseinzadeh Kassani
Hwanseong Jeong
Tavakol Nazari
Dong-Il Yeom
Kyunghwan Oh, Member, IEEE

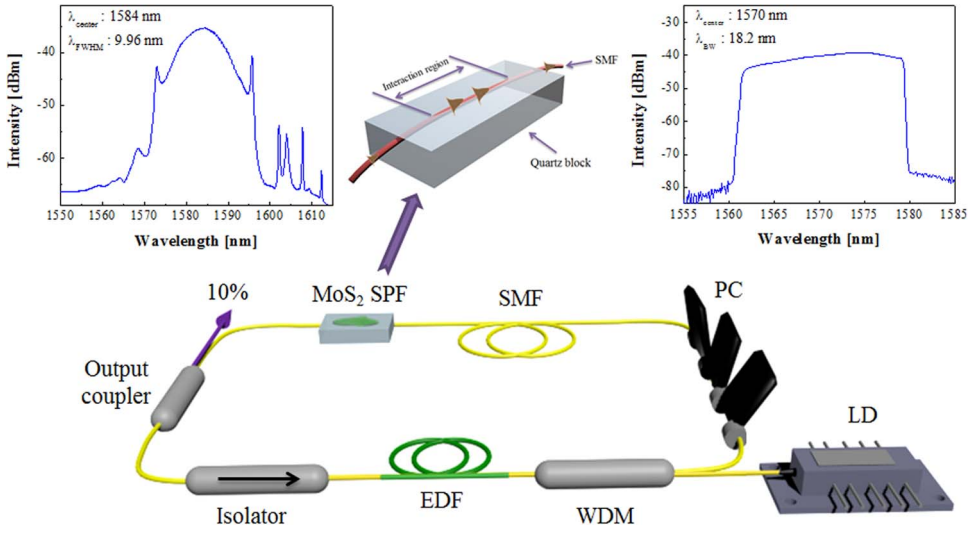

DOI: 10.1109/JPHOT.2014.2381656

Mode-Locked All-Fiber Lasers at Both Anomalous and Normal Dispersion Regimes Based on Spin-Coated MoS_2 Nano-Sheets on a Side-Polished Fiber

Reza Khazaeinezhad,[1] Sahar Hosseinzadeh Kassani,[1] Hwanseong Jeong,[2] Tavakol Nazari,[1] Dong-Il Yeom,[2] and Kyunghwan Oh,[1] *Member, IEEE*

[1]Photonic Device Physics Laboratory, Institute of Physics and Applied Physics, Yonsei University, Seoul 120 749, Korea
[2]Department of Physics and Energy Systems Research, Ajou University, Suwon 443 749, Korea

DOI: 10.1109/JPHOT.2014.2381656

Manuscript received October 22, 2014; revised November 24, 2014; accepted December 4, 2014. Date of publication December 18, 2014; date of current version January 6, 2015. Corresponding authors: D.-I. Yeom and K. Oh (e-mail: diyeom@ajou.ac.kr; koh@yonsei.ac.kr).

Abstract: We demonstrate an all-fiberized mode-locked laser by employing Molybdenum Disulfide (MoS_2) spin-coated onto a side-polished fiber (SPF) as an in-line saturable absorber. Single crystal MoS_2 has been exfoliated via the Li intercalation method and then dispersed with large population of few-layer MoS_2 nano-sheets in ethanol. Subsequently, a saturable absorber has been prepared using a relatively simple method: spin-coating the uniform MoS_2 solution on the fabricated SPF without using any polymer or toxic procedure. Power-dependent transmission property of the prepared MoS_2 nano-sheets on the SPF was experimentally analyzed, providing the feasibility to apply it as an efficient in-line saturable absorption behavior. By deploying the MoS_2 SPF into a fiber laser cavity with finely tuned laser pump power and cavity dispersion, mode-locked pulses were obtained at anomalous and normal dispersion of the laser cavity. The self-started soliton pulses at the anomalous dispersion regime were generated with a spectral bandwidth of 9.96 nm at 1584 nm and a pulse duration of 521 fs. Moreover, by managing the dispersion to the normal regime, stable pulses at net-normal intra-cavity dispersion with 11.9 ps pulse duration were obtained with a spectral bandwidth of 18.2 nm at 1570 nm. The results prove the effectiveness of developing MoS_2 saturable absorbers and applications for pulsed laser operation.

Index Terms: Molybdenum disulfide, nonlinear materials, saturable absorber, mode-locked fiber laser.

1. Introduction

Over the past few years, nanomaterials such as graphene, carbon nanotubes (CNTs), and semiconductor quantum dots have been widely investigated for their applications to lasers, optical switches, photodetectors, and solar cells [1]–[3]. In particular, the applications of graphene and CNTs as nonlinear saturable absorbers (SA) for passively mode-locked fiber lasers [4], [5], are extremely attractive for their optical uses in such fields as optical communications, optical signal processing, biology, and medicine [6]–[8]. Extensive investigations on graphene and carbon nanotubes (CNTs) have not only introduced new nanomaterials with excellent physical and

optical characteristics but have opened up the study of new 2-D materials as well. Researchers have recently started investigation on graphene analogues-materials comprising stacked atomic layers [9]. MoS_2, which is one of the transition metal dichalcogenides, is a layered material with strong in-plane bonding and weak out-of-plane interactions enabling exfoliation into two-dimensional layers [10]. There are many interesting layer-dependent properties of MoS_2, which differ greatly from the properties of the bulk material, such as valley polarization due to the electronic structure of this material [11]. In contrast to graphene, MoS_2 has a transition from an indirect band-gap in the bulk to a direct band-gap in the monolayer, with the indirect band-gap of 1.3 eV increasing to a direct band-gap of 1.8 eV [12]. The direct band-gap in monolayer MoS_2 causes significant changes in photoluminescence, photoconductivity, and absorption which open the possibility to numerous optoelectronic applications [13]–[15].

Quite recently, the ultrafast nonlinear optical properties of MoS_2 were investigated using Z-scan measurements [16]. The reported relaxation time of MoS_2 nano-sheets ($\sim$30 fs) corresponds to the intra-band transitions of the excited free carriers [16]. On the other hand, the lifetime of inter-band transitions was reported to be on the picosecond time scale for MoS_2 in few-layer form [17]. Thus, 2-D MoS_2 nano-sheets are able to serve as a saturable absorber for mode-locked ultrafast lasers [18]–[22], similarly to graphene and single-walled carbon nanotubes. Although the photoluminescent and electronic properties of MoS_2 nano-sheets have attracted worldwide attention, the pulse shaping ability of MoS_2 nano-sheets as a saturable absorber in mode-locked erbium-doped fiber lasers has not been extensively explored. The reported mode locked fiber lasers based on MoS_2 have employed fiber ferrule type saturable absorbers [19]–[21]. Although the fabrication process for fiber ferrule SAs is comparatively simple, this SA is vulnerable to destruction by mechanical damage or high power operation. Furthermore, short nonlinear interactions with materials deposited in ferrule SAs may restrict the pulse shaping ability of the material as well as the performance of the resultant lasers.

In the present study, the aforementioned issues were alleviated by using a side polished fiber (SPF) to control the interaction between light and MoS_2. Compared to fiber ferrules, the SPF has a higher damage threshold and a longer interaction length which increase the efficiency of the nonlinear effect and thereby facilitate laser mode locking. Here, high-quality few-layer MoS_2 nano-sheets were deposited on the SPF surface from an ethanol-based suspension. These high-quality nano-sheets were prepared by liquid phase exfoliation (LPE) [23], [24], and their quality was confirmed by Raman spectroscopy and transmission electron microscopy. In contrast to the use of chemical vapor deposition (CVD) for the consistent preparation of MoS_2 thin film [20], [22], the LPE method does not require the use of toxic etchants and polymers or a difficult transfer process of CVD MoS_2 film. We constructed a mode-locked fiber laser incorporating our MoS_2 deposited on side-polished fiber as a saturable absorber (MoS_2 SPF-SA). By managing the dispersion of the ring laser cavity, we obtained stable mode-locking operation at the anomalous and normal dispersion regime fiber lasers, demonstrating both femtosecond and picosecond pulses. These experimental results show that MoS_2 is a promising nonlinear optical material with applications ranging from ultra-fast laser photonics to nonlinear Kerr photonics.

2. Sample Preparation

In order to take full advantage of the optical properties of 2-D MoS_2 nano-sheets, a reliable method of producing uniform solutions of these nano-sheets is necessary. There are several methods presently available for top-down exfoliation of nano-sheets from bulk MoS_2. High-purity single-crystal flakes can be produced using mechanical cleavage methods, and these flakes are suitable for device fabrication and fundamental characterization [13]–[15]. However, this method does not allow for consistent control of the flake size or thickness. High-purity MoS_2 thin films can also be synthesized via chemical vapor deposition (CVD), but CVD is a costly method and requires difficult etching processes using toxic solutions and polymers [20], [22]. Therefore, liquid-phase methods for preparation of MoS_2 are very promising to obtain large quantities of

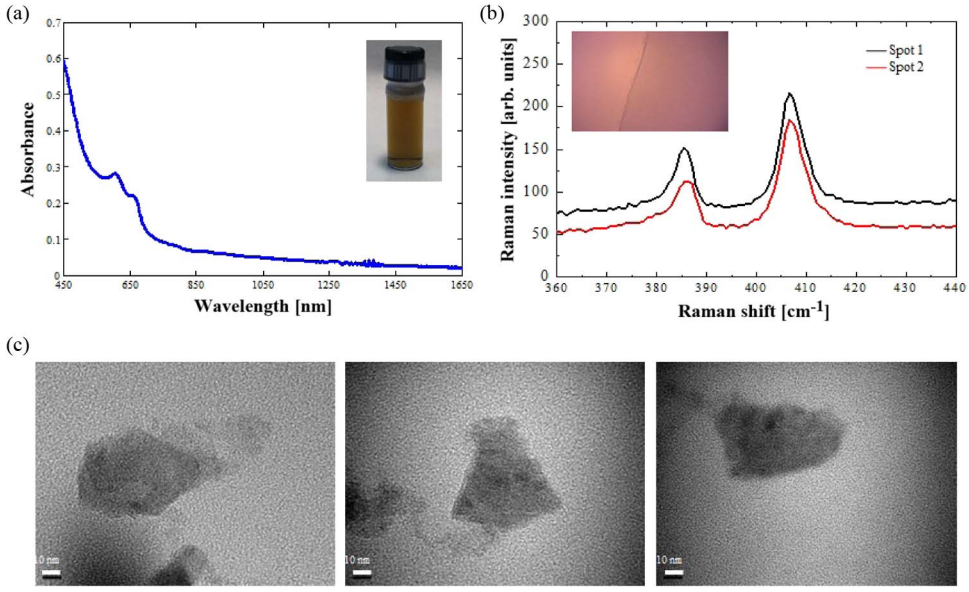

Fig. 1. (a) Linear optical absorption spectrum of the prepared solution. (Inset) Image of a uniform solution of MoS_2 nano-sheets. (b) Raman spectra of the deposited MoS_2 nano-sheets on substrate (Inset) Microscopic image of the spin coated solution on the SiO_2 substrate. (c) TEM images of the MoS_2 nano-sheets on the TEM grid.

exfoliated nano-sheets. Lithium-based chemical exfoliation has been demonstrated for MoS_2 [23], [24] which allows the layers to be exfoliated in liquid and produce high-yield sub-micrometer-sized few-layer MoS_2 nano-sheets in ethanol.

The inset of Fig. 1(a) shows a photograph of a uniform solution of MoS_2 nano-sheets in ethanol. UV-Vis-NIR transmission of a prepared solution was carried out via spectrophotometer. Fig. 1(a) demonstrates the linear optical absorption spectrum with two main peaks corresponding to exciton bands at the K-point of the Brillouin zone. Almost flat absorption in the telecommunication band characterizes the broadband optical response in the near-infrared wavelength.

The prepared solution was spin coated on SiO_2 substrate. The inset of Fig. 1(b) presents an optical image of the deposited layer on the substrate. Since each material has its own phonon modes, the Raman spectrum can be used to identify its constituents very precisely. For the Raman measurements, the 514.4 nm (2.41 eV) line of a diode-pumped-solid-state laser was used as an excitation source. The laser was focused by a 50$\times$ microscope objective lens (0.8 N.A.), and the same objective was used to collect and collimate the scattered light. The scattered signal was dispersed with a Jobin-Yvon Triax 550 spectrometer (1800 grooves/mm) and detected with a back-illuminated CCD detector. The spectral resolution was about 0.7 cm^{-1} and the laser power was kept below 0.2 mW. Fig. 1(b) depicts the phonon dispersions of MoS_2 on the substrate in two different spots. The main Raman peaks correspond to the in-plane E^1_{2g} phonon mode (409 cm^{-1}) and the out-of-plane A_{1g} mode (383 cm^{-1}) [25]. The distance between these peaks is less than that of bulk MoS_2, confirming that the deposited layer consists of few-layer MoS_2 nano-sheets. Moreover, we performed high-contrast transmission electron microscopy (TEM) of MoS_2 nano-sheets on a TEM grid. The results confirm 2-D thin nano-sheets with lateral size in the tens of nanometers as shown in Fig. 1(c). These measurements confirmed the high quality of the few-layer MoS_2 nano-sheets.

The side-polished fiber (SPF) was made from a conventional single mode optical fiber (SMF) by a precision wheel polishing method after the fiber is secured in the V-groove of a quartz block with epoxy [26]. Fig. 2(a) schematically shows the SPF with the interaction region on the surface. A D-shaped cladding structure was fabricated by removing a part of the fiber cladding,

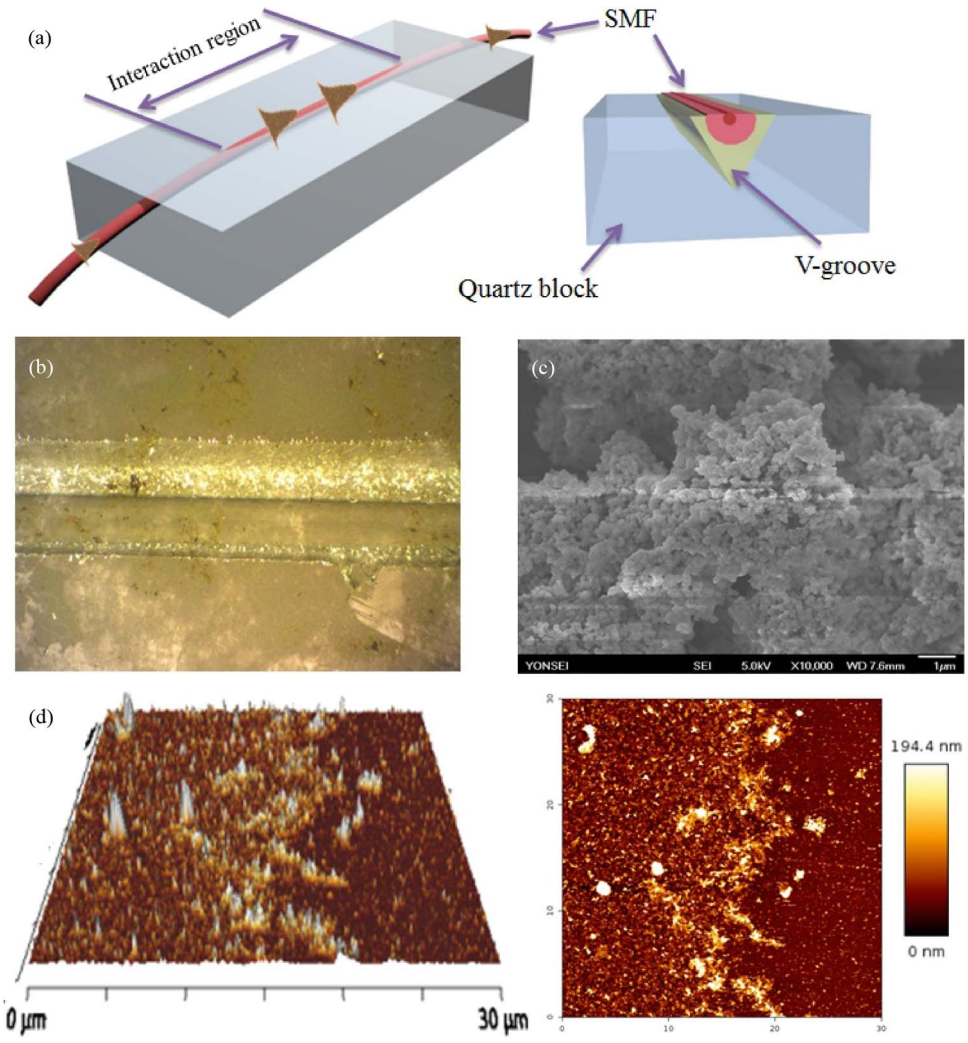

Fig. 2. (a) Schematic of the fabricated SPF and cross section view. (b) Optical microscope, (c) SEM. (d) AFM measurements of the spin-coated MoS_2 nano-sheets on SPF.

as shown in the inset of Fig. 2(a). When the optical signal launched into the optical fiber reaches the side-polished coupling region, a part of the electric field in the core evanescently interacts with the material on the polished surface. Therefore, when nonlinear materials are placed in this region, the input light can interact with the materials without significant optical loss.

The distance from the fiber core to the polished surface is determined by the insertion loss (IL) during polishing. The surface of the SPF was polished down to within a few microns of the fiber core where the initial IL was measured to be 0.16 dB with negligible polarization dependent loss (PDL). Subsequently, we deposited the MoS_2 nano-sheets on the fabricated SPF using the spin coating method. After attempting spin coating five times the prepared MoS_2 SPF-SA showed $\sim$5.5 dB IL and $\sim$4.8 dB PDL. The microscope image [see Fig. 2(b)] and SEM image [see Fig. 2(c)] of the surface of SPF confirm that the MoS_2 nano-sheets covered the entire area of the interacting region of the SPF. The thickness of the optimized MoS_2 layer deposited on the SPF was analyzed with the JPK NanoWizard atomic force microscope (AFM). Fig. 2 (d) demonstrates the 3-D and 2-D scans of 30×30 μm area on the SPF. The surface is relatively rough, since the nano-sheets are forming irregular stacks. The thickness of the deposited MoS_2 layer is $\sim$195 nm.

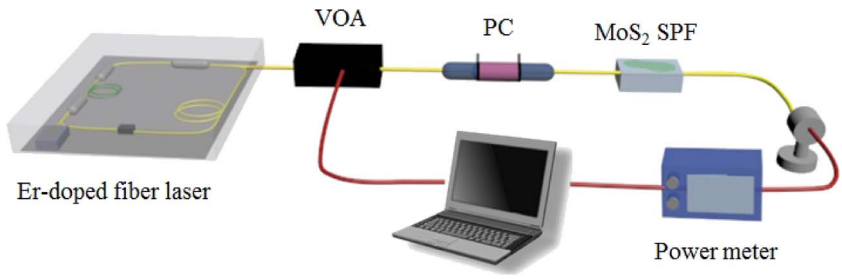

Fig. 3. Experimental set-up all fiber nonlinear transmission measurement. (VOA: variable optical attenuator, PC: polarization controller.)

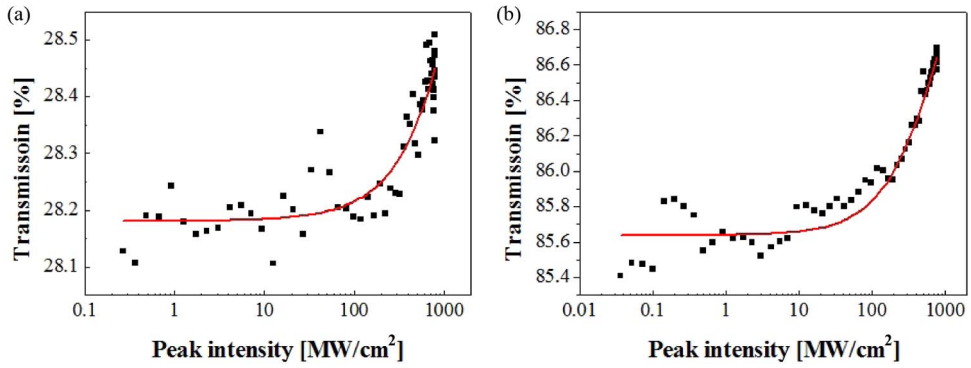

Fig. 4. Nonlinear transmission for different input polarization states. (a) Minimum transmission. (b) Maximum transmission.

3. Nonlinear Optical Characterization

In order to characterize the nonlinear optical response of the fabricated MoS_2 device, we used the transmission measurement set-up shown in Fig. 3. The optical properties of the prepared sample were characterized using a stable Er-doped optical fiber oscillator source which operates at a central wavelength of 1563 nm with pulse duration of 800 fs and a repetition rate of 41 MHz. A computer-controlled motor driven variable optical attenuator (VOA) adjusted the input optical power. The polarization of the incident light was changed via an in-line polarization controller (PC). First, a reference signal was taken, then the prepared MoS_2 SPF-SA was inserted between the PC and the power meter. Transmission was checked at the same repetition time and input power as the reference signal.

Fig. 4 depicts the results of the nonlinear transmission curves of the MoS_2 samples for the polarization states exhibiting minimum and maximum transmission. Intensity dependent transmission is observed and the measurement results are fitted to a curve modeling the two-level saturable absorber. The minimum transmission, by adjusting the polarization state, exhibited 72% initial insertion loss and the transmission increased with intensified input power, as shown in Fig. 4(a). Also, Fig. 4(b) depicts 15% initial loss when the state of input polarization is adjusted to maximum transmission. In both above cases, the MoS_2 could not be fully saturated due to limitations of the light source power.

Furthermore, to verify the measured saturable absorption characteristics of MoS_2, we re-measured these data in different ways. The input power was increased (from low to high) and decreased (from high to low); both nonlinear transmittance curves correctly almost overlap. We also tested a non-deposited side polished fiber in the nonlinear transmission setup without MoS_2 deposited, and only a flat transmission curve was observed. Based on these results, it can be concluded that the saturable absorption properties are contributed by only the MoS_2 nonlinear behavior. Thus, the optical absorption of MoS_2 nano-sheets is intensity-dependent,

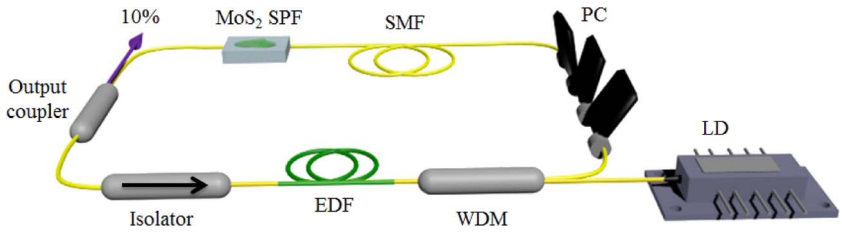

Fig. 5. Configuration of ring cavity fiber laser including the MoS2 SPF. (LD: laser diode, WDM: wavelength division multiplexer, PC: polarization controller, EDF: Erbium-doped fiber, SMF: single mode fiber).

and a suitable application is to employ MoS_2 as a saturable absorber (SA) for pulse shaping in passively mode-locked fiber lasers.

4. Mode-Locked Fiber Laser Experiment

A passive erbium-doped mode-locked fiber laser at anomalous dispersion regime was built by employing the fabricated MoS_2 SPF-SA as schematically sketched in Fig. 5. The total length of the laser cavity is estimated to be 8.20 m with a net cavity dispersion of -0.080 ps^2. A homogenous gain medium, a piece of 1.2 m highly-doped erbium-doped fiber (EDF), was pumped using a 980 nm laser diode source (LD) via a 980/1550 wavelength division multiplexing (WDM) coupler. A polarization-independent optical isolator is used to force the unidirectional operation of the ring cavity. A polarization controller is inserted to match the round-trip polarization state in the fiber ring cavity. 10% of the intra-cavity optical power is tapped via a fiber coupler and the other 90% of the lasing light is fed back into the ring cavity fiber laser. Since the dispersion value along with the nonlinearity is one of the critical factors for soliton pulse formation, the dispersion in the ring cavity is optimized by adding 2 m of extra SMF. An optical spectrum analyzer (Yokogawa AQ6370 B) with spectral resolution of 0.5 nm, an RF spectrum (Agilent technologies N9000A) with span range from 10 Hz to 10 kHz, an autocorrelator (Femtochrome; FR-103HS) with resolution of 10 fs, and a 1 GHz oscilloscope (Tektronix TDS 784 D) combined with a 12.5 GHz photodetector (EOT ET-3500F) are employed to simultaneously monitor the laser spectra and output pulses.

First, the fiber laser operation while incorporating the SPF without MoS_2 deposited was shown to be continuous-wave (CW) emission, even though the pump strength and cavity polarization were tuned. Then, the MoS_2 SPF-SA was spliced into the laser cavity and self-started passive mode-locking of the fiber laser was observed with a starting point of 74.7 mW pump power. Fig. 6 demonstrates the measured performance of the fabricated mode-locked fiber laser at anomalous dispersion regime.

Stable soliton pulses with a 3-dB spectral bandwidth of 9.96 nm at a center wavelength of 1584 nm are generated by an applied pump power of 82 mW in Fig. 6(a). The Kelly sideband in the optical spectrum indicates that soliton-like pulse was generated. The average power of the pulsed output was 0.79 mW. Pulse duration was measured using an intensity autocorrelator. The full-width half-maximum of the pulse width was 521 fs fitted by a Sech^2-shaped pulse, with background noise suppressed by 54 dB. The time trace of the oscilloscope is shown in Fig. 6(c) with a period of 39.66 ns. Fig. 6(d) and its inset depict radio frequency (RF) spectra of the generated pulse train with different spans. The pulse repetition rate of the stable laser output was measured to be 25.21 MHz, which corresponds to a laser cavity length of 8.20 m. The wide span measurement of the RF spectrum illustrates stable operation of the mode-locked laser without exhibiting a Q-switching instability. These experimental results show highly stable, passive mode locking performance of the fiber laser enabled by the MoS_2 SA.

Furthermore, mode-locked operations at net-normal intra-cavity dispersion of fiber laser were obtained by managing the intra-cavity dispersion and adding a 1.39 m dispersion

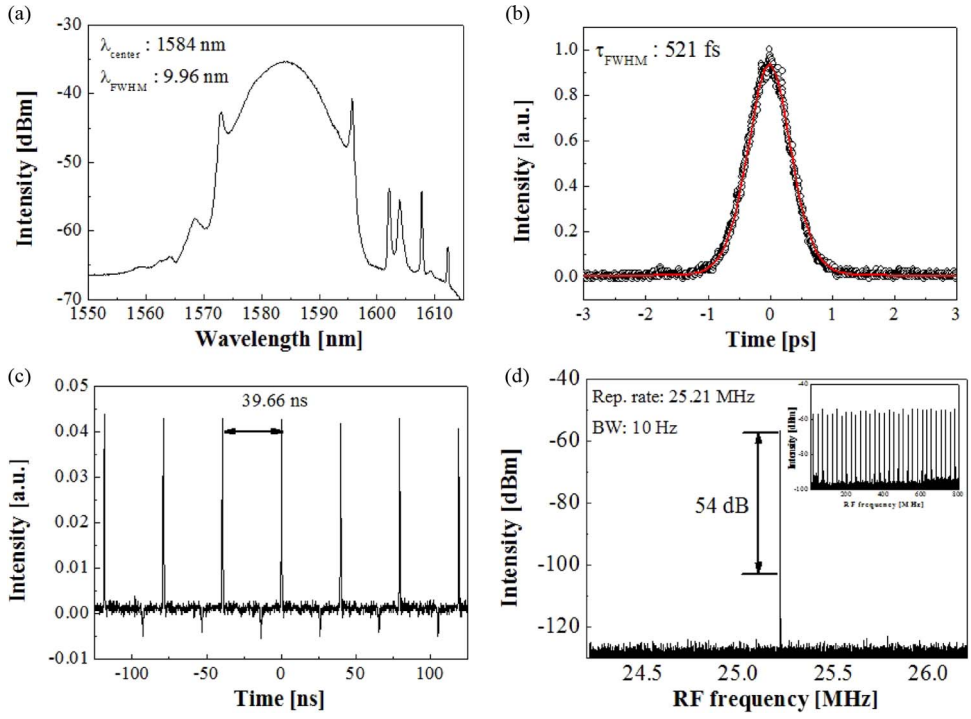

Fig. 6. Performance of the fabricated anomalous dispersion soliton mode-locking fiber laser. (a) Output optical spectrum. (b) Intensity autocorrelation trace. (c) The output pulse train. (d) RF spectrum measured around the fundamental repetition rate. (Inset: wide band RF spectrum.)

compensating fiber (DCF). The total length of the laser cavity is estimated to be 7.95 m with a net cavity dispersion of 0.095 ps^2. The output pulses at the net-normal dispersion of ring laser were simultaneously monitored. The self-started passive mode-locking fiber laser at normal intra-cavity dispersion regime were observed starting at an applied pump power of 199 mW. The laser output characteristics at the applied pump power of 241 mW are shown in Fig. 7. As shown in Fig. 7(a), the typical flat-top square shape of a soliton pulses spectrum at the normal dispersion regime is observed, where its 3-dB spectral bandwidth is 18.2 nm at a central wavelength of 1570 nm. The full-width half-maximum of the pulse width was measured to be 11.9 ps assuming a Gaussian-shaped pulse [see Fig. 7(b)]. The output pulse train is shown in the inset of Fig. 7(b).

The radio frequency (RF) spectra of the generated pulse train are shown with different spans in Fig. 7(c) and its inset. A 26.02 MHz RF signal was observed, which corresponds to the fundamental repetition rate of the length of the 7.95 m ring cavity laser. The background noise was well suppressed by 76 dB from the main peak. The wide span RF spectrum verifies stable operation of the mode locking without any Q-switching instability [see the inset of Fig. 7(c)]. By varying the input pump power, the average output power of the soliton laser at the net-normal dispersion of cavity was measured, as shown in Fig. 7(d). The stable and robust mode-locking conditions were maintained with increasing pump power until 352 mW, and did not need further adjustment of the polarization controller. These observations prove that highly stable mode-locked operation at net normal intra-cavity dispersion of fiber laser was enabled by the MoS_2 nano-sheets on SPF. The band-gap of few-layer MoS_2 sheets can reduce to 0.08 eV depends on the ratio between Mo and S ions [18]. Photons with higher energy than the band-gap excite the few-layer MoS_2 and thus electrons will be transferred from the valance band to the conduction band. The final states will be fully occupied under strong excitation and exhibited saturable absorption properties which has been confirmed by Z-scan measurements [16]. To the best of our knowledge, this is the first observation of Er-doped fiber laser using spin-coated MoS_2 nano-sheets

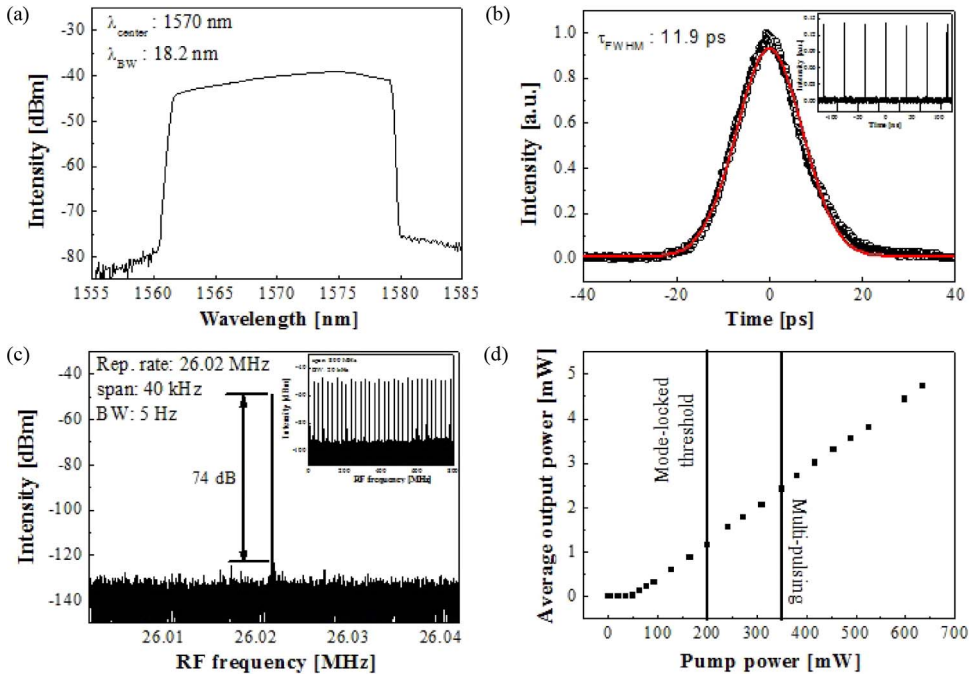

Fig. 7. Operation of normal dispersion soliton pulses from the net normal dispersion laser. (a) Optical spectrum. (b) Intensity autocorrelation function [(Inset) Pulse train]. (c) RF spectra. (d) Pump power versus laser output power measurement.

onto a side-polished fiber (SPF). Our study demonstrated that unlike to graphene and CNT, which require the use of polymers to preserve optical nonlinearity [27]–[32], MoS_2 does not need any additional polymer for stable and robust pulse generation. Also, the recent report based on Z-scan measurements demonstrated the MoS_2 nano-sheets exhibit better saturable absorption response and higher saturable carrier density than graphene [16]. Enhancing the output power is being further pursued by the authors optimizing the output coupling ratio in the fiber coupler.

5. Conclusion

In summary, we demonstrated passive harmonic Er-doped mode-locked operation at the anomalous and normal dispersion regime of fiber lasers based on a MoS_2 nano-sheet SA through evanescent wave interaction. High-quality few-layer MoS_2 nano-sheets were made in ethanol solvent via the Li intercalation method. The quality of dispersion was checked by Raman spectroscopy and TEM. The MoS_2 nano-sheets were simply spin coated on the fabricated side polished fiber and the existence of MoS_2 flakes and thickness of deposited layers on the SPF were investigated. The nonlinear optical properties of the prepared sample demonstrated the possibility of MoS_2 nano-sheets as a saturable absorber in a passive mode-locked fiber laser. An all-fiber ring cavity including the MoS_2 SPF-SA was constructed with different intra-cavity dispersions to confirm the pulse shaping ability of MoS2. In the anomalous dispersion regime, soliton-like shaped pulses were stably obtained with 521 fs pulse duration and a spectral bandwidth of 9.96 nm at 1584 nm, with a 25.21 MHz repetition rate. Subsequently, the intra-cavity dispersion of ring laser was moved to the normal regime by splicing the dispersion compensating fiber to the ring cavity. Stable and robust mode-locked pulses at net-normal intra-cavity dispersion were generated with a spectral bandwidth of 18.2 nm at 1570 nm, 11.9 ps pulse duration, and a 26.02 MHz repetition rate. Our experimental results clearly show that MoS_2 nano-sheets possess saturable absorption, which can be exploited for pulsed laser applications.

References

[1] F. Bonaccorso, Z. Sun, T. Hasan, and A. C. Ferrari, "Graphene photonics and optoelectronics," *Nat. Photon.*, vol. 4, no. 9, pp. 611–622, Aug. 2010.
[2] P. Avouris, M. Freitag, and V. Perebeinos, "Carbon-nanotube photonics and optoelectronics," *Nat. Photon.*, vol. 2, no. 6, pp. 341–350, Jun. 2008.
[3] P. V. Kamat, "Quantum dot solar cells. Semiconductor nanocrystals as light harvesters," *J. Phys. Chem. C*, vol. 112, no. 48, pp. 18 737–18 753, Oct. 2008.
[4] Q. Bao *et al.*, "Atomic layer graphene as saturable absorber for ultrafast pulsed lasers," *Adv. Funct. Mater.*, vol. 19, no. 19, pp. 3077–3083, Oct. 2009.
[5] H. Jeong *et al.*, "Ultrafast mode-locked fiber laser using a waveguide-type saturable absorber based on single-walled carbon nanotubes," *Appl. Phys. Exp.*, vol. 6, no. 5, May 2013, Art. ID. 052705.
[6] H. A. Haus, "Mode-locking of lasers," *IEEE J. Sel. Top. Quantum Electron.*, vol. 6, no. 6, pp. 1173–1185, Dec. 2000.
[7] N. Akhmediev and A. Ankiewicz, "Dissipative solitons: From optics to biology and medicine," in *Lecture Notes in Physics*, vol. 751. Berlin, Germany: Springer-Verlag, 2008.
[8] Y. Liu *et al.*, "Regenerative Er-doped fiber amplifier system for high-repetition-rate optical pulses," *J. Opt. Soc. Korea*, vol. 17, no. 5, pp. 357–361, Aug. 2013.
[9] R. Mas-Balleste, C. Gomez-Navarro, J. Gomez-Herrero, and F. Zamora, "2D materials: To graphene and beyond," *Nanoscale*, vol. 3, no. 1, pp. 20–30, Jan. 2011.
[10] K. S. Novoselov *et al.*, "Two-dimensional atomic crystals," in *Proc. Nat. Academy Sci. USA*, vol. 102, no. 30, pp. 10 451–10 453, Jul. 2005.
[11] H. Zeng, J. Dai, W. Yao, D. Xiao, and X. Cui, "Valley polarization in MoS_2 monolayers by optical pumping," *Nat. Nanotech.*, vol. 7, no. 8, pp. 490–493, Aug. 2012.
[12] L. F. Mattheis, "Band structures of transition-metal-dichalcogenide layer compounds," *Phys. Rev. B*, vol. 8, no. 8, pp. 3719–3740, Oct. 1973.
[13] A. Splendiani *et al.*, "Emerging photoluminescence in monolayer MoS_2," *Nano Lett.*, vol. 10, no. 4, pp. 1271–1275, Mar. 2010.
[14] H. S. Lee *et al.*, "MoS_2 Nanosheet phototransistors with thickness-modulated optical energy gap," *Nano Lett.*, vol. 12, no. 7, pp. 3695–3700, Jun. 2012.
[15] Z. Yin *et al.*, "Single-layer MoS_2 phototransistors," *ACS Nano.*, vol. 6, no. 1, pp. 74–80, Dec. 2011.
[16] K. Wang *et al.*, "Ultrafast saturable absorption of two-dimensional MoS_2 nanosheets," *ACS Nano.*, vol. 7, no. 10, pp. 9260–9267, Oct. 2013.
[17] R. Wang *et al.*, "Ultrafast and spatially resolved studies of charge carriers in atomically thin molybdenum disulfide," *Phys. Rev. B*, vol. 86, no. 4, Jul. 2012, Art. ID. 045406.
[18] S. Wang *et al.*, "Broadband few-layer MoS_2 saturable absorbers," *Adv. Mater.*, vol. 26, no. 21, pp. 3538–3544, Jun. 2014.
[19] H. Zhang *et al.*, "Molybdenum disulfide (MoS_2) as a broadband saturable absorber for ultra-fast photonics," *Opt. Exp.*, vol. 22, no. 6, pp. 7249–7260, Mar. 2014.
[20] H. Xia *et al.*, "Ultrafast erbium-doped fiber laser mode-locked by a CVD-grown molybdenum disulfide (MoS_2) saturable absorber," *Opt. Exp.*, vol. 22, no. 14, pp. 17 341–17 348, Jul. 2014.
[21] R. Khazaeinezhad *et al.*, "Saturable optical absorption in MoS_2 nano-sheet optically deposited on the optical fiber facet," *Opt. Commun.*, vol. 335, pp. 224–230, Jan. 2015.
[22] R. Khazaeizhad, S. Hosseinzadeh Kassani, H. Jeong, D.-I. Yeom, and K. Oh, "Mode-locking of Er-doped fiber laser using a multilayer MoS_2 thin film as a saturable absorber in both anomalous and normal dispersion regimes," *Opt. Exp.*, vol. 22, no. 19, pp. 23 732–23 742, Sep. 2014.
[23] M. B. Dines, "Lithium intercalation via n-butyllithium of layered transition-metal dichalcogenides," *Mater. Res. Bull.*, vol. 10, no. 4, pp. 287–291, Apr. 1975.
[24] J. N. Coleman *et al.*, "Two-dimensional nanosheets produced by liquid exfoliation of layered materials," *Science*, vol. 331, no. 6017, pp. 568–571, Feb. 2011.
[25] H. Li *et al.*, "From bulk to monolayer MoS_2: Evolution of Raman scattering," *Adv. Funct. Mater.*, vol. 22, no. 7, pp. 1385–1390, Apr. 2012.
[26] S.-M. Tseng and C.-L. Chen, "Side-polished fibers," *Appl. Opt.*, vol. 31, no. 18, pp. 3438–3447, Jun. 1992.
[27] H. Jeong *et al.*, "All-fiber mode-locked laser oscillator with pulse energy of 34 nJ using a single-walled carbon nanotube saturable absorber," *Opt. Exp.*, vol. 22, no. 19, pp. 22 667–22 672, Sep. 2014.
[28] G. Sobon *et al.*, "Thulium-doped all-fiber laser mode-locked by CVD-graphene/PMMA saturable absorber," *Opt. Exp.*, vol. 21, no. 10, pp. 12 797–12 802, May 2013.
[29] H. Jeong, S. Y. Choi, F. Rotermund, and D.-I. Yeom, "Pulse width shaping of passively mode-locked soliton fiber laser via polarization control in carbon nanotube saturable absorber," *Opt. Exp.*, vol. 21, no. 22, pp. 27 011–27 016, Oct. 2013.
[30] Z. Sun *et al.*, "A stable, wideband tunable, near transform-limited, graphene mode locked, ultrafast laser," *Nano Res.*, vol. 3, no. 9, pp. 653–660, Sep. 2010.
[31] S. Y. Choi, H. Jeong, B. H. Hong, F. Rotermund, and D.-I. Yeom, "All-fiber dissipative soliton laser with 10.2 nJ pulse energy using an evanescent field interaction with graphene saturable absorber," *Laser Phys. Lett.*, vol. 11, no. 1, Jan. 2014, Art. ID. 015101.
[32] T. Hasan *et al.*, "Nanotube-polymer composites for ultrafast photonics," *Adv. Mater.*, vol. 21, no. 38, pp. 3874–3899, Oct. 2009.